# Auger Electron and Photoelectron Angular Distributions from Surfaces: Importance of the Electron Source Wave

T. Greber,[a] J. Osterwalder, D. Naumović, A. Stuck, S. Hüfner,[b] and L. Schlapbach
*Institut de Physique, Université de Fribourg, Pérolles, CH-1700 Fribourg, Switzerland*
(Received 19 March 1992)

Angular distributions of Auger electrons and of photoelectrons emitted at high ($> 500$ eV) and low ($< 100$ eV) kinetic energies are compared. The high-energy patterns can be interpreted as forward-projected images of real space crystal geometry. At low energies, the angular distributions are dominated by diffraction effects, and the structural information is no longer obvious. On the other hand, the sensitivity to the geometry and the atomic composition of the surface is here dramatically enhanced. Moreover, the angular momentum character of the source wave strongly influences these patterns.

PACS numbers: 61.16.–d, 79.60.Cn

The techniques of Auger electron and photoelectron diffraction are established as valuable tools for the study of structural problems on surfaces [1,2]. The advantages of these methods arise from their sensitivity to the atomic species under investigation and from a relative ease of interpretation of the measured diffraction patterns. This second property is restricted to electron energies above 300 eV and originates from the fact that the differential elastic scattering cross sections are dominated by the forward-scattering amplitudes [1,2]. This gives rise to characteristic maxima in directions parallel to near-neighbor bonds. As a consequence, the character of the *source wave*, i.e., the wave of the excited electron prior to crystal diffraction, is of minor importance in this regime. This is no longer true at low kinetic energies. Recent experimental findings [3,4] reveal that here the simple forward-scattering scheme cannot be applied. In this Letter, we demonstrate that one of the major needs is to take into account the source wave character explicitly.

In an elegant experiment, Frank *et al.* [3] measured the complete angular distribution of Auger electrons emitted at 65 eV kinetic energy from the (111) face of a Pt single crystal. Among others, they recognized how valuable such $2\pi$ intensity maps are to explore the physics and chemistry of surfaces [4–10]. In order to draw quantitative conclusions, however, such measurements have to be compared with an appropriate theory. Frank *et al.* [3,4] described these angular distributions, which in this particular case show intensity dips along major interatomic axes, as containing the "silhouettes" of near-surface atoms "back lit" by Auger emission originating from atoms deeper in the solid. They in fact concluded that hitherto these intensity variations had been mistakenly attributed to elastic scattering and diffraction among other processes. This provoked a series of Comments which defended the established theories [11–14].

In pursuing an understanding of these experiments. Terminello and Barton have presented new data [15] which indicate that the low kinetic energy by itself cannot explain the intensity dips along interatomic axes. As was found before, e.g., by McDonnell, Woodruff, and Holland [16], they observe a *minimum* in Cu $M_{2,3}M_{4,5}M_{4,5}$ emission along the [001] direction from a Cu(001) surface. On the other hand, they show that the Cu $3p$ photoelectron flux from the same sample and at the same energy exhibits a *maximum* along [001]. This led them to the conclusion that the dips are not caused by any scattering effect at all and that the character of the source wave may influence the diffraction pattern. This same conclusion had been reached earlier by Aberdam *et al.* [17]. We would like to illustrate here the present understanding of these effects.

We first discuss the high-energy case and compare in Fig. 1 two stereographically projected photoelectron and Auger electron $2\pi$ scans from Cu(001) at kinetic energies of 808 eV (Cu $2p_{3/2}$) and 840 eV (Cu $LMM$) [18]. The diffraction patterns are very similar and consequently not very sensitive to the source wave character. Maxima occur along ⟨011⟩ nearest-neighbor directions as well as along the [001] next-nearest-neighbor direction. A second phenomenon is the appearance of well-defined sets of bands that are centered at positions that correspond to projections of high-density (111) and (001) crystal planes [Fig. 1(c)]. They seem to be of a similar origin as the Kikuchi bands known in electron microscopy [19] that have been observed quite early also in Auger electron spectroscopy [20]. Based on these experimental findings, one might to first order neglect diffraction and broadly interpret such data as projections of nuclear charge onto the hemisphere above the surface [1,2,6–9], although a precise analysis must involve a full model calculation [1].

In going to low kinetic energies, the situation becomes more complex, and the obvious structural information is reduced to the *symmetries* of the surface under investigation. This does not mean that such patterns are insensitive to the atomic *structure* of the surface. On the contrary, it turns out that diffraction patterns of low-energy photoelectrons or Auger electrons are an excellent probe for surface structure. In order to demonstrate this, we compare in Fig. 2 high- and low-energy diffraction patterns of Cu emission from two similar crystalline surfaces: Cu(001) and $Cu_3Au(001)$. In both systems the atoms occupy the sites of a face-centered-cubic (fcc) lattice, with lattice constants of 3.61 Å (Cu) and 3.75 Å

© 1992 The American Physical Society 

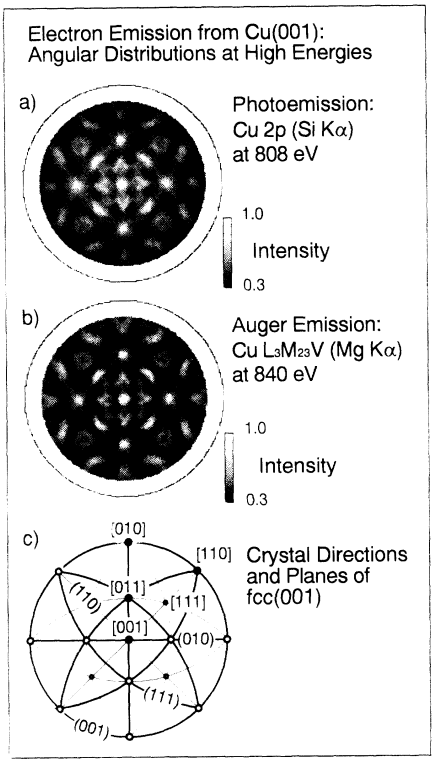


FIG. 1. Stereographically projected electron diffraction patterns at high kinetic energies. The electron intensities have been measured starting from 78° off the surface normal, and are given in a linear gray scale. (a) Si $K\alpha$ excited Cu $2p_{3/2}$ photoelectron diffraction pattern at 808 eV. (b) Mg $K\alpha$ excited Cu $LMM$ Auger electron diffraction pattern at 840 eV. (c) Map of all principal high atomic density axes and planes of a face-centered-cubic (fcc) crystal projected on the hemisphere above the (001) face.

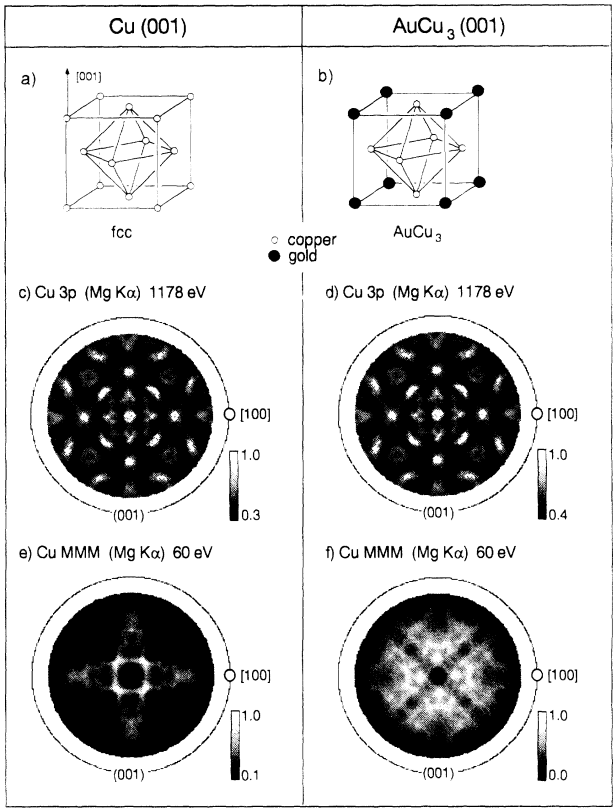


FIG. 2. Comparison of the sensitivity of high- and low-energy diffraction to the atomic structure of surfaces: (a) Schematic representation of the unit cell of a face-centered-cubic (fcc) Cu(001) surface. (b) Same as (a) but for a $Cu_3Au(001)$ surface. (c) Mg $K\alpha$ excited Cu $3p$ (1178 eV) photoelectron diffraction pattern from Cu(001) and (d) from $Cu_3Au(001)$. (e) Cu $MMM$ (60 eV) Auger electron diffraction pattern from Cu(001) and (f) from $Cu_3Au(001)$. All data are given in the stereographic projection, using a linear gray scale.

($Cu_3Au$). In the ordered bulk phase of $Cu_3Au$ ($T < 663$ K), the cube corners are occupied by gold atoms and the face centers by Cu atoms [Fig. 2(b)]. Our measurements were done at room temperature, in which case the (001) surface is known to be terminated by a mixed and ordered Cu-Au layer, while the second layer contains only Cu atoms [21]. From Figs. 2(c) and 2(d), it is evident that the structural differences between the two surfaces are only weakly, if at all, reflected in the high-energy diffraction patterns. The Cu $3p$ (1178 eV) patterns in both cases mainly show the signature of the fcc arrangement of atoms, no matter what atomic type or lattice constant.

In strong contrast, the diffraction patterns of the Cu $MMM$ transition at a low kinetic energy of 60 eV [Figs. 2(e) and 2(f)] are found to be significantly different for the two surfaces. This striking sensitivity to bond length and atomic type of scattering atoms bears the promise of a very powerful structural tool, similar to low-energy electron diffraction (LEED), but with additional chemical discrimination. The tradeoff we have to make in comparison with high-energy photoelectron or Auger electron diffraction is that the structural information is here much less obvious, and that a rigorous theoretical description is needed. One of the main reasons for the complications in the low-energy case is that forward scattering is no longer dominant, and that at the same time the wavelength of the probing electrons approaches the size of the atoms. Diffraction affects the intensity distributions strongly. In addition, the character of the source wave has to be described properly for a correct interpretation [10,17].

The angular momentum character of a photoelectron or an Auger electron depends on the particular transition involved: Parity as well as total angular momentum have to be conserved. In photoelectron diffraction experiments with x-ray excitation, the photon polarization is more or less confined to a plane (unpolarized radiation) or to a particular direction (polarized radiation). Selection rules cause the source wave to be anisotropic for all photoelectrons as well as for all Auger electrons which do not form

a pure $s$ wave and whose initial ion (before the Auger recombination) is not spherically symmetric, i.e., does not have a total angular momentum of $J=\frac{1}{2}$ [22]. This makes the analysis of data such as those presented by Frank *et al.* [3,4] and Terminello and Barton [15] or those in Figs. 2(e) and 2(f) quite involved.

Here, we shall illustrate the influence of the angular momentum character of the source wave, although an exact calculation, taking multiple scattering into account, is beyond the scope of this work. In fact, we shall not even introduce the above-mentioned anisotropic emission. Following the suggestion of Aberdam *et al.* [17], we have performed single-scattering calculations [23] with the electron source wave described as isotropic spherical waves with $s$, $p$, $d$, $f$, $g$, or $h$ character, i.e., with the angular momentum quantum number $l$ taking values of 0, 1, 2, 3, 4, or 5. This is done by summing incoherently the single-scattering intensities within a suitable cluster for all $2l+1$ different magnetic sublevels $m$ for a given angular momentum $l$. All parameters except $l$ were kept constant between the different simulations. Figure 3 indicates how strongly the diffraction patterns at such low energies are affected by the angular momentum character of the source wave. The physics behind this strong $l$ dependence, even for isotropic emitters, lies in the strong anisotropy of the individual magnetic sublevel waves. Important scattering atoms in the photoelectron near field either are "illuminated" by or are near a node of such a sublevel wave, and contribute accordingly to the total wave interference. The simulations for Cu-*MMM* in Fig. 3 show clearly that a mainly $s$-wave scattering process yields a "peak" along the [001] direction of Cu(001) while $f$-wave scattering yields a "dip." Thus, the well-established theory can produce "peaks" and "dips" within the same formalism. The above implies that no simple rules, as, e.g., even or odd parity, determine whether a maximum or a minimum occurs along particular internuclear axes. We note that the Cu $3p$ photoemission data of Terminello and Barton [15], which involve a large portion of $s$-wave emission [24], show indeed a maximum along [001]. Their Auger data show a dip along this same direction which is consistent with mainly $f$-wave emission: It is well known that in the atomic $M_{23}M_{45}M_{45}$ Cu([Ar] $3s^2 3p^5 3d^{10} 4s^1$) to Cu([Ar] $3s^2 3p^6 3d^8 4s^1$) $+e_{\text{Auger}}$ decay, the $l=3$ character dominates, while the $l=1$ and $l=5$ channels are strongly suppressed [17]. Although this Auger transition involves two valence states ($3d$), it can be expected to retain more or less the same atomic source wave character. This same argument should, by the way, hold also for the comparison of the Auger data from Cu(001) and $Cu_3Au$(001).

In order to make a quantitative comparison with such low-energy Auger data, multiple-scattering events should be taken into account, which is beyond our means. Furthermore, if the Auger transition involves different angular momentum channels, interference between these channels needs to be considered although the relative phases are often not known at this point. We therefore keep the comparison at this qualitative level which still indicates the essential ingredients that a full interpretation of low-energy data must contain.

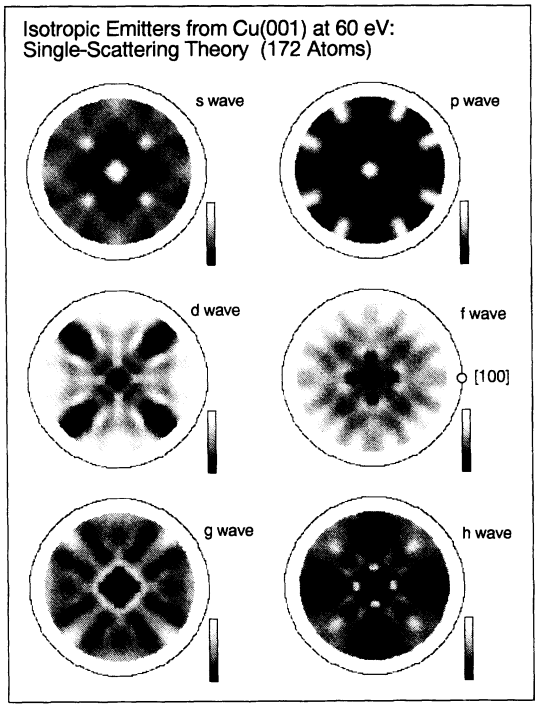


FIG. 3. Single-scattering calculations for isotropic electron source waves emanating from Cu atoms within a Cu(001) surface. The spherical-wave scattering code of Friedman and Fadley [23] has been slightly modified to generate this type of source wave. At low kinetic energies (60 eV) the crystal lattice strongly discriminates different angular momenta ($s$,$p$,$d$,$f$,$g$, $h$) of the outgoing electrons. All other parameters have been kept constant between different simulations.

In summary, we have demonstrated that current diffraction theories that contain a proper description of the *angular momentum character* of the outgoing electron wave [23] can well reproduce Auger electron *as well as* photoelectron diffraction phenomena at high *and* low kinetic energies. While the interpretation of high-energy diffraction data is rather straightforward, low energies require a detailed calculation and the knowledge of the matrix elements involved in the particular transition. We have furthermore shown that the structural sensitivity of such patterns is strongly enhanced at low energies. A full theoretical understanding of these phenomena is important not only for structural studies, but also for quantitative chemical analysis of single crystal surfaces [25].

This work was supported by the Schweizerischen Nationalfonds. One of the authors (S.H.) appreciates the warm hospitality extended to him by the group "Physique

des Solides" of the Institut de Physique of the Université de Fribourg.

---

[a]Current address: Fritz-Haber-Institut der Max-Planck-Gesellschaft, Faradayweg 4-6, D-1000 Berlin 33, Germany.

[b]Permanent address: Fachbereich Physik, Universität des Saarlandes, D-6600 Saarbrücken, Germany.

[1] C. S. Fadley, in *Synchrotron Radiation Research: Advances in Surface Science,* edited by R. Z. Bachrach (Plenum, New York, 1992), Chap. 11.

[2] W. F. Egelhoff, Jr., Crit. Rev. Solid State Mat. Sci. **16**, 213 (1990).

[3] D. G. Frank, N. Battina, R. Golden, F. Lu, and A. T. Hubbard, Science **247**, 182 (1990).

[4] D. G. Frank, T. Golden, O. M. R. Chyan, and A. T. Hubbard, J. Vac. Sci. Technol. A **9**, 1254 (1991).

[5] R. J. Baird, C. S. Fadley, and L. F. Wagner, Phys. Rev. B **15**, 666 (1977).

[6] H. Li and B. P. Tonner, Phys. Rev. B **37**, 3959 (1988).

[7] M. Seelmann-Eggebert and H. J. Richter, J. Vac. Sci. Technol. B **9**, 1861 (1991).

[8] Z.-L. Han, S. Hardcastle, G. R. Harp, H. Li, X.-D. Wang, J. Zhang, and B. P. Tonner, Surf. Sci. **258**, 313 (1991).

[9] J. Osterwalder, T. Greber, A. Stuck, and L. Schlapbach, Phys. Rev. B **44**, 13764 (1991).

[10] T. Greber, J. Osterwalder, S. Hüfner, and L. Schlapbach, Phys. Rev. B **45**, 4540 (1992).

[11] S. A. Chambers, Science **248**, 1129 (1990).

[12] W. F. Egelhoff, Jr., J. W. Gadzuk, C. J. Powell, and M. A. Van Hove, Science **248**, 1129 (1990).

[13] X. D. Wang, Z. L. Han, B. P. Tonner, Y. Chen, and S. Y. Tong, Science **248**, 1129 (1990).

[14] D. P. Woodruff, Science **248**, 1131 (1990).

[15] L. J. Terminello and J. J. Barton, Science **251**, 1281 (1991).

[16] L. McDonnell, D. P. Woodruff, and B. W. Holland, Surf. Sci. **51**, 249 (1975).

[17] D. Aberdam, R. Baudoing, E. Blanc, and C. Gaubert, Surf. Sci. **71**, 279 (1978).

[18] D. Naumović, A. Stuck, T. Greber, J. Osterwalder, and L. Schlapbach (to be published).

[19] H. Bethge, in *Electron Microscopy in Solid State Physics,* edited by J. Heydenreich (Elsevier, Amsterdam, 1987).

[20] T. W. Rusch, J. P. Bertino, and W. P. Ellis, Appl. Phys. Lett. **23**, 359 (1973).

[21] T. M. Buck, G. H. Wheatley, and L. Marchat, Phys. Rev. Lett. **51**, 43 (1983).

[22] W. Mehlhorn, in *Atomic Inner Shell Physics,* edited by B. Crasemann (Plenum, New York, 1985).

[23] D. J. Friedman and C. S. Fadley, J. Electron Spectrosc. Relat. Phenom. **51**, 689 (1990).

[24] S. M. Goldberg, C. S. Fadley, and S. Kono, J. Electron Spectrosc. Relat. Phenom. **21**, 285 (1981).

[25] H. E. Bishop, Surf. Interface Anal. **15**, 27 (1990); **16**, 118 (1990).

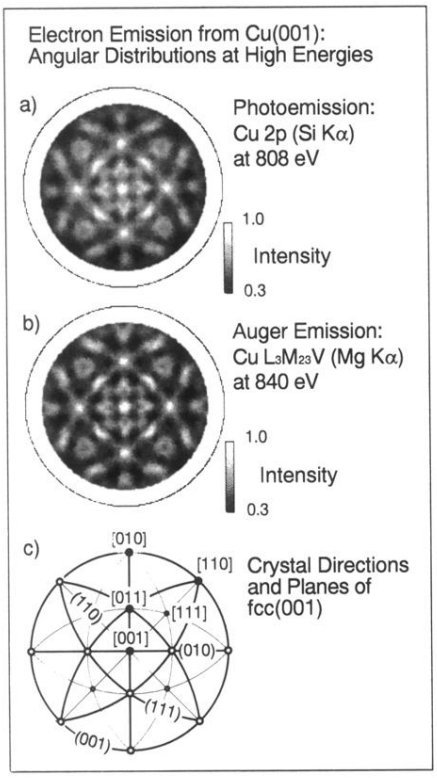


FIG. 1. Stereographically projected electron diffraction patterns at high kinetic energies. The electron intensities have been measured starting from 78° off the surface normal, and are given in a linear gray scale. (a) Si $K\alpha$ excited Cu $2p_{3/2}$ photoelectron diffraction pattern at 808 eV. (b) Mg $K\alpha$ excited Cu $LMM$ Auger electron diffraction pattern at 840 eV. (c) Map of all principal high atomic density axes and planes of a face-centered-cubic (fcc) crystal projected on the hemisphere above the (001) face.

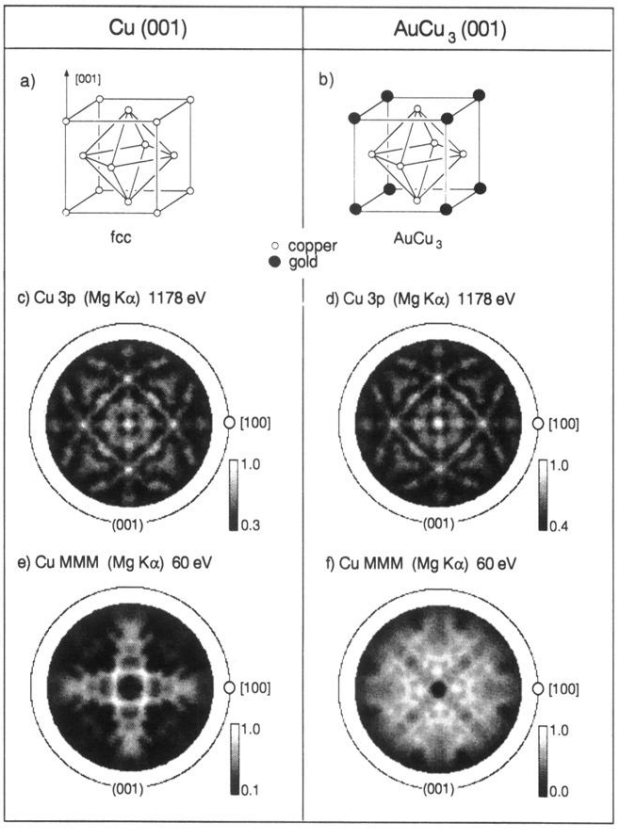


FIG. 2. Comparison of the sensitivity of high- and low-energy diffraction to the atomic structure of surfaces: (a) Schematic representation of the unit cell of a face-centered-cubic (fcc) Cu(001) surface. (b) Same as (a) but for a $Cu_3Au(001)$ surface. (c) Mg $K\alpha$ excited Cu $3p$ (1178 eV) photoelectron diffraction pattern from Cu(001) and (d) from $Cu_3Au(001)$. (e) Cu $MMM$ (60 eV) Auger electron diffraction pattern from Cu(001) and (f) from $Cu_3Au(001)$. All data are given in the stereographic projection, using a linear gray scale.

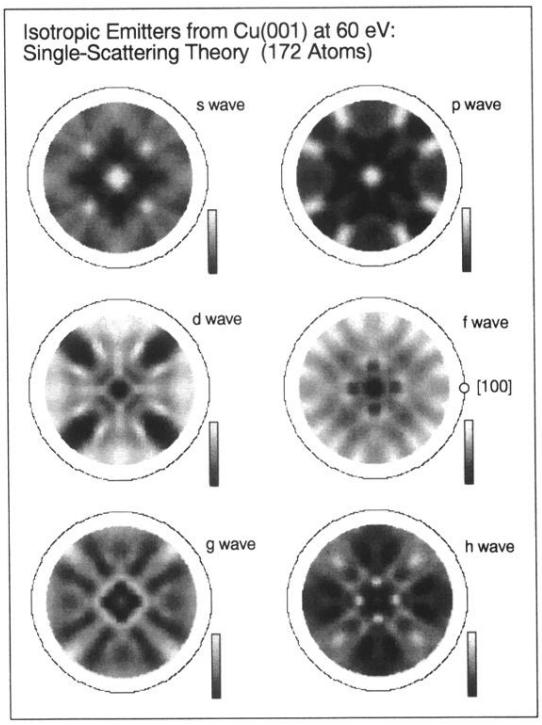


FIG. 3. Single-scattering calculations for isotropic electron source waves emanating from Cu atoms within a Cu(001) surface. The spherical-wave scattering code of Friedman and Fadley [23] has been slightly modified to generate this type of source wave. At low kinetic energies (60 eV) the crystal lattice strongly discriminates different angular momenta ($s$,$p$,$d$,$f$,$g$, $h$) of the outgoing electrons. All other parameters have been kept constant between different simulations.